E-ISSN: 2707-8299
P-ISSN: 2707-8280
www.civilengineeringjournals.com/ijsde
IJSDE 2024; 5(2): 43-51
Received: 02-07-2024
Accepted: 03-08-2024

Vincenzo De Luca
Department D.I.S., University of Basilicata, Viale dell'Ateneo Lucano 10, Potenza 85100, Italy

Cosimo Marano
S.A.F.E., University of Basilicata, Viale dell'Ateneo Lucano 10, Potenza 85100, Italy

Corresponding Author:
Vincenzo De Luca
Department D.I.S., University of Basilicata, Viale dell'Ateneo Lucano 10, Potenza 85100, Italy

A finite element method with inter-element interpolation points for thin plate. Part I: Compatible formulation

Vincenzo De Luca and Cosimo Marano

DOI: https://doi.org/10.22271/27078280.2024.v5.i2a.35

Abstract
In this study, an inter-element point interpolation is introduced within a displacement-based formulation of the Finite Element Method (FEM) to analyze elastic thin plates. The problem domain is discretized using a mesh of rectangular elements, where the deflection field is the sole primary variable. The displacement field is interpolated using quadratic functions, with the flexibility to customize these functions by adjusting the positions of control points either within, along the borders, or outside the mesh elements. This approach ensures continuity between adjacent elements and reduces the overall degrees of freedom in the governing discretized equations. A weak formulation is employed to derive the system of discretized equations, incorporating both displacement and rotational boundary conditions. The FEM formulation is implemented in a computational framework to solve the static problem of an elastic thin plate under a specified load. Numerical applications are conducted to evaluate the performance of the proposed model on isotropic, linear elastic thin plates. The results indicate that the model can accurately reproduce both displacement and moment fields, demonstrating good agreement with corresponding analytical solutions.

Keywords: Finite element method, elastic analysis of thin plate, element interpolation points, bending thin plate

Introduction
The analysis of thin plates has attracted significant attention due to its wide applications in civil and industrial engineering (Zienkiewicz and Taylor, 2000a, 2000b) [1, 2]. Over the years, numerous classical thin plate elements have been developed to address these challenges. Among the early contributions, the Morley element (Morley, 1971) [3] stands out for its computational efficiency, with only six degrees of freedom per element. Hybrid stress models (Allwood and Cornes, 1969) [4] offer higher accuracy but are computationally demanding, rendering them impractical for widespread use.In recent decades, the development of high-performance finite elements (Leonetti and Aristodemo, 2015; Bilotta and Casciaro, 2007) [5, 6] has become a central theme in the literature. To address the modeling of thin and thick plates (Boussem *et al*., 2020) [7] and shells (Rebiai *et al*., 2014) [8], strain-based finite element methods have been proposed, which derive the displacement field from the strain field. However, the most commonly adopted approach in traditional Finite Element Method (FEM) continues to rely on compatible elements with numerical integration performed at Gauss points.
Although alternative frameworks using mixed or generalized variational principles have been extensively explored, many of these methods, particularly those employing high-degree interpolations (Zienkiewicz and Taylor, 2000a, 2000b) [1, 2], suffer from shear locking and spurious zero-energy solutions in thin structure analysis. Strategies to mitigate these issues, including reduced integration techniques for shear terms and specialized plate elements, have been proposed. However, their complexity and computational demands limit their adoption in most FEM codes. Despite the substantial progress in modeling elastic solids using conventional FEM elements, the issue of ensuring continuity between elements has received less attention. This is particularly important in thin plate analysis, which requires the continuity of both deflection and its derivatives. Achieving such continuity often necessitates high-order interpolation and integration, significantly increasing computational complexity.
This paper introduces a straightforward compatible FEM formulation for thin plates,

designed for ease of implementation and characterized by its reliance on simplified assumptions for displacement and derived fields. A novel thin plate element based on an inter-element continuity technique is proposed. Using the weak form principle of the equilibrium equation, a discrete formulation is developed, employing bi-quadratic interpolation functions that ensure continuity of both the displacement field and its derivatives.

To validate the proposed model, numerical applications are performed on two load cases: a uniformly distributed load and a central point load. Also, two boundary conditions are analyzed: a simply supported plate and a fully clamped plate. The numerical results are evaluated against the corresponding analytical solutions.

Materials and Methods

Theory

The present numerical study focuses on modeling the bending behavior of thin plates based on Kirchhoff's theory. The system is treated as a two-dimensional domain representing a homogeneous, isotropic, linear-elastic material.

A Cartesian coordinate system (O, x, y, z) is employed, where the x and y axes lie in the mid-plane of the plate, and the $z-axis$ is perpendicular to it (Figure 1). The plate has a thickness h, a volume domain V, and a boundary surface S, and it is subjected to a transverse load $p(x,y)$. Plate bending is described in terms of the transverse displacement $u_z(x,y)$, with shear deformations assumed negligible (Szilard, 1974; Timoshenko and Woinowsky-Krieger, 1984) [9, 10]. The following kinematic assumptions are made:

- the normals to the mid-plane remain straight and undistorted, with zero transverse shear strains γ_{zx} and γ_{zy};
- the extensional deformations ε_{xx} and ε_{yy} are linearly distributed through the thickness and vanish at the mid-plane;
- the transverse displacement $u_z(x,y)$ along the z-axis is infinitesimally small;
- the normal stress component σ_{zz} is negligible compared to the in-plane stress components σ_{xx} and σ_{yy}.

The compatibility equations are determined as follows. The rotations are obtained as partial derivatives of the transverse displacement:

$$\varphi_x = -\frac{\partial u_z}{\partial x}, \quad (1)$$

$$\varphi_y = -\frac{\partial u_z}{\partial y}. \quad (2)$$

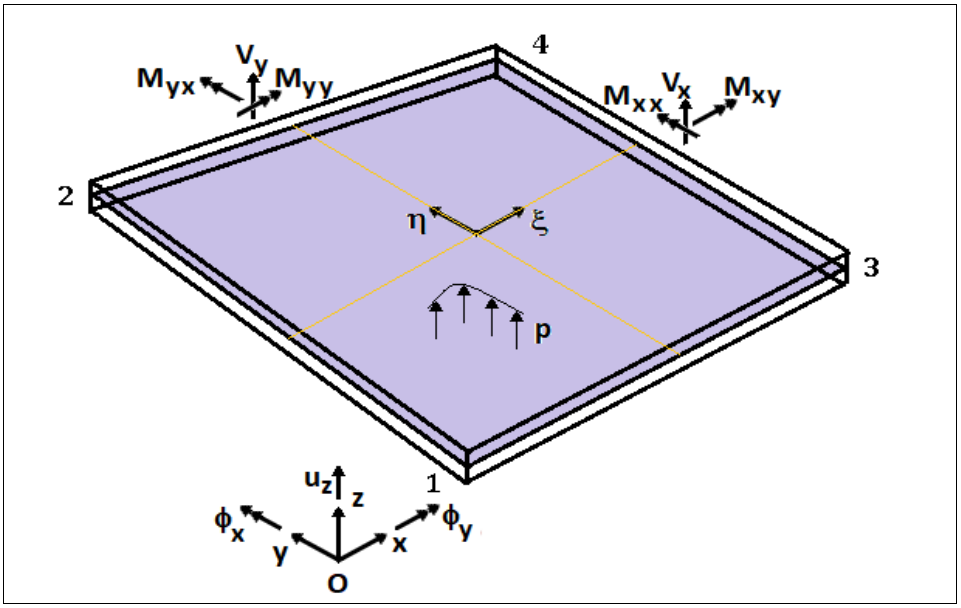

Fig 1: Variables of the Kirchhoff plate defined within the reference coordinate system.

The displacement components u_x and u_y in the x and y directions, respectively, are expressed as:

$$u_x = -z \cdot \varphi_x = -z \cdot \frac{\partial u_z}{\partial x}, \quad (3)$$

$$u_y = -z \cdot \varphi_y = -z \cdot \frac{\partial u_z}{\partial y}, \quad (4)$$

where

u_z is the vertical deflection, and

φ_x and φ_y represent the rotations about the x and y axes, respectively.

The strain components are expressed as:

$$\varepsilon_{xx} = \frac{\partial u_x}{\partial x} = -z \cdot \frac{\partial^2 u_z}{\partial x^2}, \quad (5)$$

$$\varepsilon_{yy} = \frac{\partial u_y}{\partial y} = -z \cdot \frac{\partial^2 u_z}{\partial y^2} \quad (6)$$

$$\gamma_{xy} = \frac{\partial u_x}{\partial y} + \frac{\partial u_y}{\partial x} = -2 \cdot z \cdot \frac{\partial^2 u_z}{\partial x \partial y} \quad (7)$$

For a linear isotropic elastic material, the stress components are defined as:

$$\sigma_{xx} = \frac{E}{1-\upsilon^2} \cdot (\varepsilon_{xx} + \upsilon \cdot \varepsilon_{yy}) = -\frac{E}{1-\upsilon^2} \cdot z \cdot \left(\frac{\partial^2 u_z}{\partial x^2} + \upsilon \cdot \frac{\partial^2 u_z}{\partial y^2}\right) \quad (8)$$

$$\sigma_{yy} = \frac{E}{1-\upsilon^2} \cdot (\upsilon \cdot \varepsilon_{xx} + \varepsilon_{yy}) = -\frac{E}{1-\upsilon^2} \cdot z \cdot \left(\upsilon \cdot \frac{\partial^2 u_z}{\partial x^2} + \frac{\partial^2 u_z}{\partial y^2}\right), \quad (9)$$

$$\sigma_{xy} = \frac{E}{2 \cdot (1+\upsilon)} \cdot \gamma_{xy} = -\frac{E}{1-\upsilon^2} \cdot z \cdot \frac{\partial^2 u_z}{\partial x \partial y}. \quad (10)$$

The bending moments are determined by integrating the stress components across the thickness of the plate:

$$M_{xx} = \int_{-\frac{h}{2}}^{\frac{h}{2}} \sigma_x \cdot z \cdot dz = -\frac{E \cdot h}{12 \cdot (1-\upsilon^2)} \cdot \left(\frac{\partial^2 u_z}{\partial x^2} + \upsilon \cdot \frac{\partial^2 u_z}{\partial y^2}\right), \quad (11)$$

$$M_{yy} = \int_{-\frac{h}{2}}^{\frac{h}{2}} \sigma_y \cdot z \cdot dz = -\frac{E \cdot h}{12 \cdot (1-\upsilon^2)} \cdot \left(\upsilon \cdot \frac{\partial^2 u_z}{\partial x^2} + \frac{\partial^2 u_z}{\partial y^2}\right), \quad (12)$$

$$M_{xy} = \int_{-\frac{h}{2}}^{\frac{h}{2}} \sigma_x \cdot z \cdot dz = -\frac{E \cdot h}{12 \cdot (1-\upsilon^2)} \cdot (1-\upsilon) \cdot \frac{\partial^2 u_z}{\partial x \partial y}. \quad (13)$$

The shear forces are obtained from the rotational equilibrium equations:

$$V_x = -\frac{E \cdot h}{12 \cdot (1-\upsilon^2)} \cdot \left(\frac{\partial^3 u_z}{\partial x^3} + \frac{\partial^3 u_z}{\partial x \partial y^2}\right), \quad (14)$$

$$V_y = -\frac{E \cdot h}{12 \cdot (1-\upsilon^2)} \cdot \left(\frac{\partial^3 u_z}{\partial x^2 \partial y} + \frac{\partial^3 u_z}{\partial y^2 \partial x}\right). \quad (15)$$

The equilibrium equation governing the plate domain is:

$$\frac{\partial^4 u_z}{\partial x^4} + 2 \cdot \frac{\partial^4 u_z}{\partial x^2 \partial y^2} + \frac{\partial^4 u_z}{\partial y^4} = \frac{p}{D} \quad (16)$$

where D is the flexural rigidity, defined as:

$$D = \frac{E \cdot h^3}{12 \cdot (1-\upsilon^2)} \quad (17)$$

where E and υ denote the elastic modulus and Poisson's ratio, respectively.

Model construction

An elastic thin plate, defined by its volume V and boundary surface S, is considered. The plate is subjected to a volumetric body force $\underline{r}$, a surface traction $\bar{\underline{t}}$ on the free boundary S_{σ}, and imposed displacements $\bar{\underline{u}}$ on the constrained boundary $S_{\underline{u}}$. The two-dimensional static elasticity problem is governed by the equilibrium equation within the domain V, bounded by S:

$$\frac{\partial \boldsymbol{\sigma}}{\partial \underline{x}} + \underline{p} = \underline{0} \text{ in } V \quad (18)$$

where the stress tensor $\boldsymbol{\sigma}$ satisfies the symmetry condition:

$$\boldsymbol{\sigma}^T = \boldsymbol{\sigma}. \quad (19)$$

The boundary conditions are:

$$\boldsymbol{\sigma} \cdot \underline{n} = \bar{\underline{t}} \text{ on the free part } S_{\sigma} \text{ and} \quad (20)$$

$$\underline{u} = \bar{\underline{u}} \text{ on } S_{\underline{u}}, \quad (21)$$

where $\underline{n}$ is the unit outward normal.

The constitutive relationship for an elastic linear material is expressed as:

$$\boldsymbol{\sigma} = \mathbb{C} \cdot \boldsymbol{\varepsilon}, \quad (22)$$

Where

$$\mathbb{C} = \frac{E}{(1-\upsilon^2)} \cdot \begin{bmatrix} 1 & \upsilon & 0 \\ \upsilon & 1 & 0 \\ 0 & 0 & \frac{1-\upsilon}{2} \end{bmatrix}$$

is the elastic stiffness matrix, (23)

with its symmetry properties:

$$\mathbb{C}^T = \mathbb{C}. \quad (24)$$

The strain tensor $\boldsymbol{\varepsilon}$, also symmetric, is expressed as:

$$\boldsymbol{\varepsilon} = \frac{1}{2} \cdot \left[\left(\frac{\partial \underline{u}}{\partial \underline{x}}\right) + \left(\frac{\partial \underline{u}}{\partial \underline{x}}\right)^T\right] = \frac{\partial u}{\partial x}. \quad (25)$$

To analyze the plate's mechanical behavior, the finite element model (FEM) is constructed using the principle of virtual displacement. Key variables in the formulation include: The displacement vector $\underline{u} = [u_z]$, The bulk load vector $\underline{p} = [p]$,

the surface load vector $\bar{\underline{t}} = [t]$.

The weak form of the equilibrium equation, derived by applying the principle of virtual work, is formulated as:

$$\int_V \boldsymbol{\sigma} \cdot \delta\boldsymbol{\varepsilon} \cdot dV - \int_V \underline{p}^T \cdot \delta\underline{u} \cdot dV - \int_{S_\sigma} \underline{\bar{t}}^T \cdot \delta\underline{u} \cdot dS = 0 \quad (26)$$

It will satisfy the equilibrium equation (18) and also the boundary conditions (20) and (21), where $\delta\underline{u}$ represents an admissible variation of the displacement field satisfying $\delta\underline{u} = \underline{0}$ on ${}^tS_{\underline{u}}$, and

$\delta\boldsymbol{\varepsilon} = \frac{1}{2} \cdot \left[\left(\frac{\partial \delta\underline{u}}{\partial \underline{x}}\right) + \left(\frac{\partial \delta\underline{u}}{\partial \underline{x}}\right)^T\right] = \frac{\partial \delta\underline{u}}{\partial \underline{x}}$ is the virtual variation of the strain tensor. (27)

Also, the term present in the (26) becomes:

$$\boldsymbol{\sigma} \cdot \delta\boldsymbol{\varepsilon} = \boldsymbol{\sigma} \cdot \frac{\partial \delta\underline{u}}{\partial \underline{x}} = \mathbb{C}_e \cdot \frac{\partial \underline{u}}{\partial \underline{x}} \cdot \frac{\partial \delta\underline{u}}{\partial \underline{x}} \quad (28)$$

Discretized finite element equations

The displacement field at any point $\underline{x}$ is interpolated as:

$$\underline{u}(\underline{x}) = \mathbf{A}(\xi, \eta) \cdot \underline{U} \quad (29)$$

Where

n is the number of discrete points;

$\underline{U}$ is the vector of unknown nodal displacement;

$\underline{x}$ is the vector of coordinates of an arbitrary point in the domain;

$\boldsymbol{A}$ is the matrix containing the shape functions, which links the displacement $\underline{u}$ of the current point with the global vector $\underline{U}$ of the nodal parameters.

Similarly, the virtual displacement field is expressed as:

$$\delta\underline{u}(\underline{x}) = \mathbf{A}(\xi, \eta) \cdot \delta\underline{U} \quad (30)$$

Substituting the interpolated field (29) into the virtual work equation (26) the discrete FEM formulation becomes:

$$\int_V \mathbb{C} \cdot \frac{\partial \mathbf{A}}{\partial \underline{x}} \cdot \underline{U} \cdot \frac{\partial \mathbf{A}}{\partial \underline{x}} \cdot \delta\underline{U} \cdot dV - \int_V \underline{p}^T \cdot \mathbf{A} \cdot \delta\underline{U} \cdot dV - \int_{S_\sigma} \underline{\bar{t}}^T \cdot \mathbf{A} \cdot \delta\underline{U} \cdot dS = 0 \quad (31)$$

The virtual work equation (31) can be rewritten in matrix form as:

$$\left(\mathbf{K} \cdot \underline{U} - \underline{F}\right) \cdot \delta\underline{U} = 0 \quad (32)$$

Where

$\mathbf{K} = \int_V \mathbb{C} \cdot \frac{\partial \mathbf{A}}{\partial \underline{x}} \cdot \frac{\partial \mathbf{A}}{\partial \underline{x}} \cdot dV$ is the global stiffness matrix, (33)

$\underline{P} = \int_V \underline{p}^T \cdot \mathbf{A} \cdot dV + \int_{S_\sigma} \underline{\bar{t}}^T \cdot \mathbf{A} \cdot dS$ is the global force vector. (34)

The virtual work equation (32) must be satisfied for any $\delta\underline{U}$.

$\delta\underline{U} = \underline{0}$ results for nodes on $S_{\underline{u}}$, where $\underline{U} = \bar{\underline{U}}$ must be, $\bar{\underline{U}}$ being the constrained nodal vector of displacements at boundary.

So the equation (32), being valid for each arbitrary value of $\delta\underline{U} \neq 0$, must result:

$$\mathbf{K} \cdot \underline{U} - \underline{P} = \underline{0}, \quad (35)$$

This results in a system of n linear equations with n unknowns, corresponding to the nodal displacement components represented by the vector $\underline{U}$.

The global stiffness matrix K and the force vector $\underline{F}$ are assembled by summing contributions from individual elements, following standard FEM procedures. The resulting system of linear equations is solved using appropriate numerical methods to compute the nodal displacements.

Interpolation of the transverse displacement with quadratic elements

To construct the discrete model, the matrix A is tailored specifically for bending plates, where only the transverse displacement component $u_z(x, y)$, directed along the $z - axis$, is considered.

As depicted in Figures 1 and 2, the physical domain is divided into a rectangular grid with mesh sizes $a \times b$, where each element's geometry is defined by the coordinates $x_i, y_i, i = 1,2,3,4$, corresponding to the nodes of the element. A local reference frame with coordinates ξ and η, centered at the element's center, is used as dimensionless coordinates for the element:

$$\xi = \frac{x}{a}, \quad (36)$$

$$\eta = \frac{y}{b}. \quad (37)$$

The matrix A for a generic element depends on the nine nodal parameters $U_{11}, U_{12}, \ldots U_{33}$ of the element and its adjacent elements, as:

$$\mathbf{A}(\xi, \eta) \cdot \underline{U} = u_z(\xi, \eta) = \sum_{i=1}^{3} \sum_{i=1}^{3} \phi_i(\xi) \cdot \phi_j(\eta) \cdot U_{ij} \quad (38)$$

Where the one-dimensional shape functions $\phi_i(\xi)$ and

$\phi_j(\eta)$ depend on the dimensionless coordinates ξ and η, which describe the position of the nodal parameters relative to the center of the element. In this work, we consider ξ and η equal to $\frac{1}{2}$ and 0 at a boundary edges.

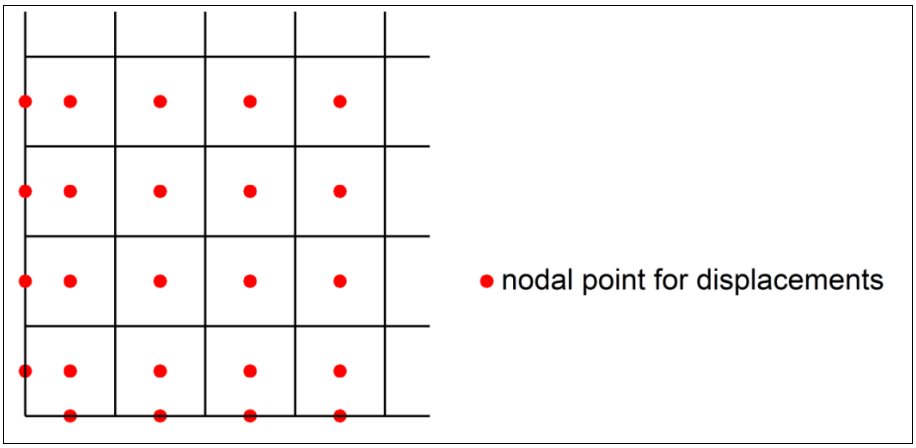

Fig 2: Schematic representation of the mesh with nodal points for displacement.

Imposing boundary conditions

Boundary conditions are directly imposed on the nodal displacements for the displacement field. For rotations, boundary conditions are expressed in terms of the nodal displacements as follows:

$$\varphi_x(\xi,\eta) = -\frac{\partial u_z}{\partial \xi} = -\sum_{j=1}^{3}\sum_{i=1}^{3}\frac{\partial \phi_i(\xi)}{\partial \xi}\cdot\phi_j(\eta)\cdot U_{ij}, \quad (39)$$

$$\varphi_y(\xi,\eta) = -\frac{\partial u_z}{\partial \eta} = -\sum_{j=1}^{3}\sum_{i=1}^{3}\phi_i(\xi)\cdot\frac{\partial \phi_j(\xi)}{\partial \eta}\cdot U_{ij}, \quad (40)$$

Numerical analysis

The formulation described above is implemented in a computational software to perform numerical analysis of classic problems involving square plates with varying boundary conditions, including fully supported and fully clamped sides. The analysis considers both uniformly distributed and centrally concentrated loads.

Square plate

A square plate with dimensions $a = 1000\ mm$ and $b = 1000\ mm$ is analyzed. The thickness of the plate is specified as $h = 2\ mm$. The material properties are given by an elastic modulus $E = 2.1 \cdot 10^4\ daN/mm^2$ and a Poisson's ratio $\upsilon = 0.3$.

Results and Discussion

Tables 1 to 4 present significant quantities, such as displacement and moment at the center and at the midpoint of the edges, for a fully clamped plate. To evaluate the performance of the FEM formulation, the numerical results obtained using the proposed model are compared with those derived from the analytical theory for bending plates. Specifically, for the simply supported plate, the double Fourier series is employed up to the eleventh term, while for the other boundary condition, a simpler approach using only the first term is utilized. The tables are organized according to the mesh refinement levels to assess the impact of mesh variation, with respect to convergence toward the reference values.

Table 1 presents results for a square plate simply supported under a uniform load. The dimensionless values and the relative errors in the central deflection and the central moment are provided. Also, the moment at the middle edge is reported, which should theoretically be zero. The graphs in Figures 3 and 4 show the convergence trends of the relative error between the numerical and reference values for the central deflection and central moment, respectively, with monotonic convergence toward the reference solution. Despite using a limited number of points, the thin plate elements yield highly accurate results, with relative errors of 0.03% for deflection and 1.11% for the central moment for a 26 x 26 mesh.

Table 2 reports results for a simply supported plate subjected to a point load at the center. The bending moment at the center is dimensionless, being normalized by dividing by a small surface area to avoid singular values. The dimensionless values, along with the corresponding relative errors, for both the central deflection and central moment are presented. The moment at the middle edge, which is expected to be zero, is also reported. For a 26 x 26 mesh, the relative errors are 0.46% for deflection and 0.44% for the central moment, even with a reduced number of points.

Table 3 provides results for a square plate fully clamped under a uniform load. The dimensionless values, along with the associated relative errors, for the central deflection, central moment, and the moment at the mid-edge are provided. The relative errors are 0.11% for deflection, 1.27% for the central moment, and 15.27% for the moment at the middle edge. The latter error remains relatively high, even with a 26 x 26 mesh.

Table 1: Square plate supported on four edges, subjected to uniform load.

Mesh	d.o.f.	o	$\alpha/(\alpha-\alpha_a)$	f	$\beta/(\beta-\beta_a)$	١	γ/γ_i
6x6	64	0.004028	-0.0084	0.047460	-0.0195	0.014425	0.2980
8x8	100	0.004043	-0.0046	0.047656	-0.0154	0.011443	0.2364
10x10	144	0.004050	-0.0029	0.047742	-0.0137	0.009477	0.1958
12x12	196	0.004054	-0.0020	0.047787	-0.0127	0.008085	0.1670
14x14	256	0.004056	-0.0014	0.047814	-0.0122	0.007049	0.1456
16x16	324	0.004058	-0.0011	0.047831	-0.0118	0.006247	0.1291
18x18	400	0.004059	-0.0008	0.047843	-0.0116	0.005609	0.1159
20x20	484	0.004059	-0.0006	0.047851	-0.0114	0.005090	0.1052
22x22	576	0.004060	-0.0005	0.047857	-0.0113	0.004658	0.0962
24x24	676	0.004060	-0.0004	0.047862	-0.0112	0.004294	0.0887
26x26	784	0.004061	-0.0003	0.047866	-0.0111	0.003982	0.0823

Dimensionless values: o the deflection at the central plate; f the moment at the central point and ١ the moment at the mid support along x (or y), and their relative errors respect to the analytical values α_a, β_a and γ_a, respectively.

Analytical values: $\alpha_a = \frac{w_c}{\left[\frac{p\cdot(a\cdot b)^2}{D}\right]} = 0.004062$, $\beta_a = \frac{M_c}{\left[\frac{p\cdot(a\cdot b)}{D}\right]} = 0.048403$, $\gamma_a = \frac{M_s}{\left[\frac{p\cdot(a\cdot b)}{D}\right]} = 0$,

where: $p = 0.001\ daN/mm^2$ is the uniformly distributed load; w_c is the displacement at the central point; M_c is the moment at the central point along x (or y); M_s is the moment at the mid edge along x (or y).

Table 4 presents results for a fully clamped plate subjected to a point load at the center. The dimensionless values and relative errors for the central deflection and moment at the middle edge are reported, while the dimensionless central moment is not computed due to its singular nature at the center. The thin plate elements deliver highly accurate results, with relative errors of 0.91% for deflection and 0.76% for the moment at the middle edge for a 26 x 26 mesh.

These results demonstrate the efficacy of the proposed method in providing accurate solutions, particularly for the deflection of the simply supported square plate under uniform load (Figure 5). The accuracy of the current results closely approaches the analytical solutions, validating the robustness of the FEM model for bending plate problems.

Table 2: Square plate supported on four edges, subjected to central point load.

Mesh	d.o.f.	o	$\alpha/(\alpha-\alpha_a)$	f	$\beta/(\beta-\beta_a)$	١	γ/γ_i
6x6	64	0.010926	-0.0581	0.025813	-0.4610	-0.001207	-0.0252
8x8	100	0.011184	-0.0359	0.030000	-0.3736	-0.000833	-0.0174
10x10	144	0.011315	-0.0245	0.033303	-0.3046	-0.000653	-0.0136
12x12	196	0.011392	-0.0179	0.036024	-0.2478	-0.000535	-0.0112
14x14	256	0.011441	-0.0137	0.038337	-0.1995	-0.000455	-0.0095
16x16	324	0.011474	-0.0109	0.040346	-0.1576	-0.000396	-0.0083
18x18	400	0.011498	-0.0088	0.042122	-0.1205	-0.000350	-0.0073
20x20	484	0.011515	-0.0073	0.043713	-0.0873	-0.000314	-0.0066
22x22	576	0.011528	-0.0062	0.045153	-0.0572	-0.000285	-0.0060
24x24	676	0.011539	-0.0053	0.046469	-0.0297	-0.000261	-0.0055
26x26	784	0.011547	-0.0046	0.047681	-0.0044	-0.000241	-0.0050

Dimensionless values: o the deflection at the central plate; f the moment at the central point and ١ the moment at the mid support along x (or y), and their relative errors respect to the analytical values α_a, β_a and γ_a, respectively.

Analytical values: $\alpha_a = \frac{w_c}{\left[\frac{P\cdot(a\cdot b)}{D}\right]} = 0.01160$, $\beta_a = \frac{M_c}{\left[\frac{P\cdot(a\cdot b)}{D}\right]} = 0.047892$, $\gamma_a = \frac{M_s}{\left[\frac{P\cdot(a\cdot b)}{D}\right]} = 0$,

where: $P = 100\ daN$ is the central point load; w_c is the displacement at the central point; M_c is the moment at the central point along x (or y), by referring F to a small area; M_s is the moment at the mid edge along x (or y).

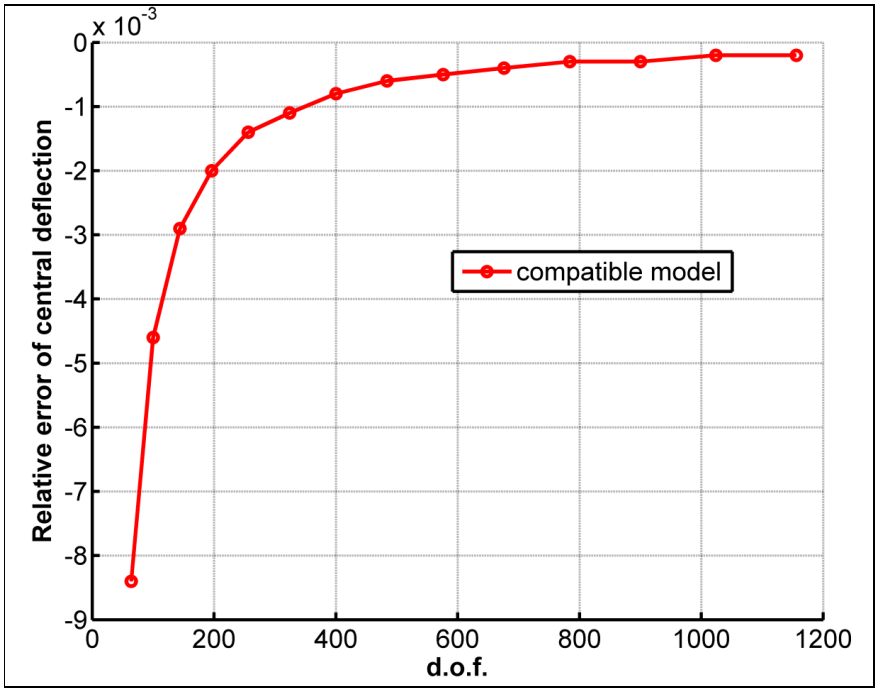

Fig 3: The relative error versus degree of freedom (d.o.f.) of central deflection for simply supported square plate uniformly loaded.

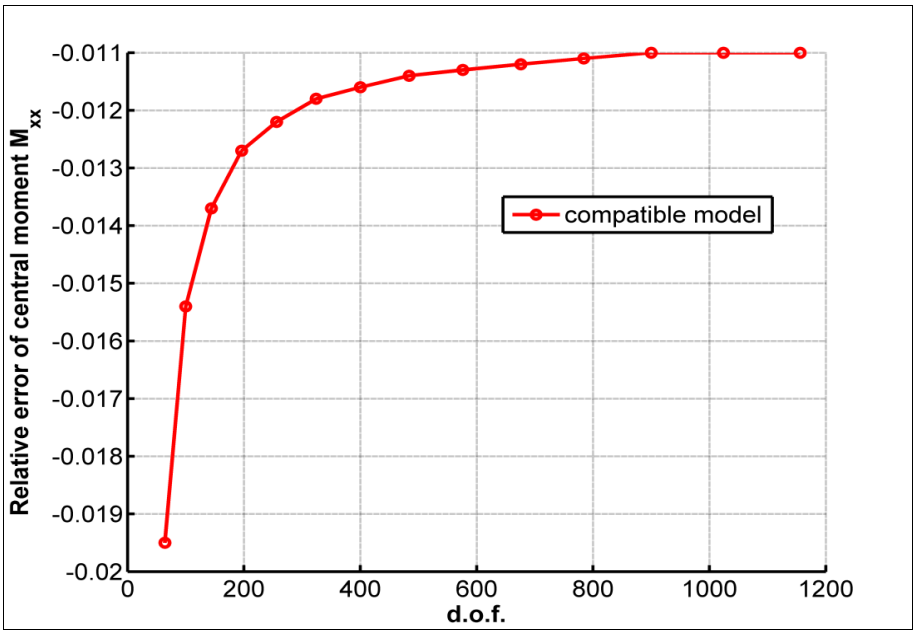

Fig 4: The relative error versus degree of freedom (d.o.f.) of central moment M_{xx} for simply supported square plate uniformly loaded.

Table 3: Square plate clamped on four edges, subjected to uniform load.

Mesh	d.o.f.	o	$\alpha/(\alpha-\alpha_a)$	ß	$\beta/(\beta-\beta_a)$	)	γ/γ_i
6x6	64	0.001141	-0.0947	0.021817	-0.0572	-0.024281	-0.5268
8x8	100	0.001195	-0.0516	0.022286	-0.0369	-0.029558	-0.4239
10x10	144	0.001220	-0.0315	0.022508	-0.0273	-0.033127	-0.3544
12x12	196	0.001234	-0.0206	0.022629	-0.0221	-0.035696	-0.3043
14x14	256	0.001242	-0.0140	0.022702	-0.0189	-0.037632	-0.2666
16x16	324	0.001248	-0.0098	0.022750	-0.0169	-0.039142	-0.2371
18x18	400	0.001251	-0.0068	0.022782	-0.0155	-0.040353	-0.2135
20x20	484	0.001254	-0.0047	0.022806	-0.0145	-0.041346	-0.1942
22x22	576	0.001256	-0.0032	0.022823	-0.0137	-0.042174	-0.1781
24x24	676	0.001257	-0.0020	0.022836	-0.0131	-0.042875	-0.1644
26x26	784	0.001259	-0.0011	0.022846	-0.0127	-0.043477	-0.1527

Dimensionless values: o the deflection at the central plate; β the moment at the central point and) the moment at the mid support along x (or y), and their relative errors respect to the analytical values α_e, β_e and γ_e, respectively.

Analytical values: $\alpha_a = \frac{w_c}{\left[\frac{p\cdot(a\cdot b)^2}{D}\right]} = 0.00126$, $\beta_a = \frac{M_c}{\left[\frac{p\cdot(a\cdot b)}{D}\right]} = 0.02314$, $\gamma_a = \frac{M_s}{\left[\frac{p\cdot(a\cdot b)}{D}\right]} = -0.05130$,

where: $p = 0.001\ daN/mm^2$ is the uniformly distributed load; w_c is the displacement at the central point; M_c is the moment at the central point along x (or y); M_s is the moment at the mid edge along x (or y).

Table 4: Square plate clamped on four edges, subjected to central point load.

Mesh	d.o.f.	o	$\alpha/(\alpha-\alpha_a)$	ß	$\beta/(\beta-\beta_a)$	¹	γ/γ_a
6x6	64	0.004773	-0.1476	-	-	-0.088844	-0.2932
8x8	100	0.005102	-0.0889	-	-	-0.099546	-0.2081
10x10	144	0.005267	-0.0595	-	-	-0.106501	-0.1527
12x12	196	0.005362	-0.0425	-	-	-0.111494	-0.1130
14x14	256	0.005422	-0.0318	-	-	-0.115250	-0.0831
16x16	324	0.005462	-0.0247	-	-	-0.118184	-0.0598
18x18	400	0.005490	-0.0196	-	-	-0.120541	-0.0410
20x20	484	0.005511	-0.0158	-	-	-0.122478	-0.0256
22x22	576	0.005527	-0.0130	-	-	-0.124097	-0.0128
24x24	676	0.005539	-0.0108	-	-	-0.125471	-0.0018
26x26	784	0.005549	-0.0091	-	-	-0.126652	0.0076

Dimensionless values: o the deflection at the central plate; ß the moment at the central point and ¹ the moment at the mid support along x (or y), and their relative errors respect to the analytical values α_a, β_a and γ_a, respectively.

Analytical values: $\alpha_a = \frac{w_c}{\left[\frac{P\cdot(a\cdot b)}{D}\right]} = 0.00560$, $\gamma_a = \frac{M_s}{\left[\frac{p\cdot(a\cdot b)}{D}\right]} = -0.1257$,

where: $P = 100\ daN$ is the central point load; w_c is the displacement at the central point; M_s is the moment at the mid edge along x (or y).

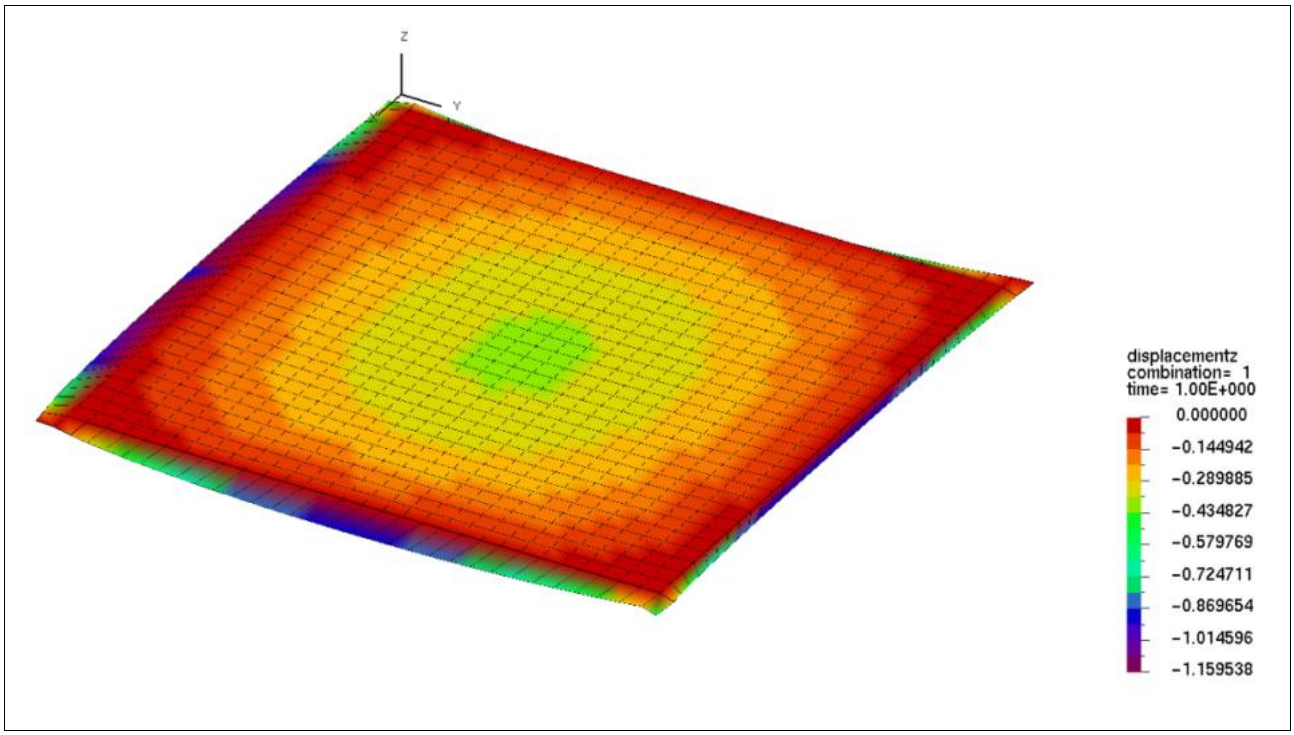

Fig 5: Color-map of the mesh, visualized as a deformed configuration, displaying the displacement z field (deflection) for a mesh 32 x 32

Conclusions

This paper presents a novel thin plate element theory based on inter-element continuity interpolation, offering an efficient solution for thin plate problems. The proposed method uses deflection as the primary field variable, which results in a reduced system stiffness matrix and consequently lower computational costs.

Numerical applications reveal that as the discretization mesh is refined, the displacement values converge rapidly toward the exact solution, stabilizing with negligible errors. Similarly, the moments exhibit a clear convergence toward their exact values, with progressively smaller deviations as the mesh is refined.

The proposed method proves to be highly accurate, particularly in predicting displacements, though it is somewhat less precise for moment predictions in thin plate analysis. Its simplicity and effectiveness make it an attractive approach for future studies on plate and shell problems of dynamic.

Acknowledgments
Vincenzo De Luca has developed the theoretical formulation, the Finite Element Method model and is author of the software code. Cosimo Marano has contributed to the elaboration of the numerical results.

References

1. Zienkiewicz O, Taylor R. The Finite Element Method. Volume 1: The Basis. Butterworth-Heinemann, Oxford; c2000a.
2. Zienkiewicz O, Taylor R. The Finite Element Method. Volume 2: Solid Mechanics. Butterworth-Heinemann, Oxford; c2000b.
3. Morley LSD. The constant-moment plate-bending element. Journal of Strain Analysis. 1971;6(1):20–24.
4. Alwood RJ, Cornes GMM. A polygonal finite element for plate bending problems using the assumed stress approach. International Journal for Numerical Methods in Engineering. 1969;1(2):135–149.
5. Leonetti L, Aristodemo M. A composite mixed finite element model for plane structural problems. Finite Elements in Analysis and Design. 2015;94:33–46.
6. Bilotta A, Casciaro R. A high-performance element for the analysis of 2D elastoplastic continua. Computer Methods in Applied Mechanics and Engineering. 2007;196(4–6):818–828.
7. Boussem F, Belounar L. A Plate Bending Kirchhoff Element Based on Assumed Strain Functions. Journal of Solid Mechanics. 2020, 12(4).
8. Rebiai C, Belounar L. An effective quadrilateral membrane finite element based on the strain approach. Measurement. 2014;50:263–269.
9. Szilard R. Theory and Analysis of Plates: Classical and Numerical Methods. Englewood Cliffs, NJ: Prentice-Hall, Inc.; c1974. p. 728.
10. Timoshenko SP, Woinowsky-Krieger S. Theory of Plates and Shells. McGraw-Hill, New York; c1984.